

## Molecular Phosphorescence in Polymer Matrix with Reversible Sensitivity

Hongwei Wu,<sup>†</sup> Long Gu,<sup>†</sup> Glib V. Baryshnikov,<sup>‡,§</sup> Hou Wang,<sup>†</sup> Boris F. Minaev,<sup>‡,§</sup> Hans Ågren,<sup>‡,Δ,\*</sup>

Yanli Zhao<sup>†,\*</sup>

<sup>†</sup>Division of Chemistry and Biological Chemistry, School of Physical and Mathematical Sciences, Nanyang Technological University, 21 Nanyang Link, 637371, Singapore

E-mail: zhaoyanli@ntu.edu.sg

<sup>‡</sup>Division of Theoretical Chemistry and Biology, School of Biotechnology, KTH Royal Institute of Technology, SE-10691 Stockholm, Sweden. E-mail: hagen@kth.se

<sup>§</sup>Department of Chemistry and Nanomaterials Science, Bogdan Khmelnytsky National University, Cherkasy 18031, Ukraine.

<sup>Δ</sup>College of Chemistry and Chemical Engineering, Henan University, Kaifeng, Henan 475004, P. R. China

**Abstract:** Ultralong organic phosphorescence strongly depends on the formation of aggregation, while it is difficult to obtain in dilute environments on account of excessive internal and external molecular motions. Herein, ultralong single molecule phosphorescence (USMP) at room temperature was achieved in the monomer state by coassembling biphenyl and naphthalene derivatives at low density with polyvinyl alcohol (PVA), where PVA provides a confined environment to stabilize the triplet state. Various factors that affect the USMP were studied, including aggregation, conformation, temperature and moisture. In these systems, the formation of

aggregates through intermolecular stacking and hydrogen bonding interactions in the film or crystal phases completely suppresses the USMP. However, the fluorescence is enhanced when coassembling these compounds at high concentration with PVA, and becomes stronger in their powder state, indicating that the intersystem crossing process is blocked by the aggregation. Theoretical calculations suggest that the aggregation depresses spin-orbit coupling between the excited singlet and triplet states and enhances nonradiative quenching process. Moreover, relatively twisted conformation is more conducive to the occurrence of intersystem crossing than planar conformation. The USMP shows delicate and reversible sensitivity to the changes of temperature and moisture, rendering them with the applicability as smart organic optoelectronic materials.

**Keywords:** polymer matrix, reversible sensitivity, self-assembly, single molecule phosphorescence, ultralong organic phosphorescence

## **Introduction**

Ultralong organic phosphorescence (UOP) has long been considered difficult to achieve at room temperature owing to the quenching of the triplet excitation induced by surrounding media.<sup>1</sup> Thus, several strategies have been developed to realize UOP, which include heavy atom effect,<sup>2-6</sup> crystal engineering,<sup>7-9</sup> host-guest doping,<sup>10</sup> and polymer dispersion.<sup>11-17</sup> Crystal engineering seems particularly promising for obtaining UOP,<sup>18-30</sup> since the suppression of nonradiative relaxation can be acquired in a rigid crystal environment by intermolecular stacking with restricted molecular vibrations and rotations.<sup>31</sup> For example, closed stacking interaction can lead to the formation of *H*-aggregation in a crystal phase in order to stabilize the triplet state for UOP.<sup>32</sup> Bright UOP was

achieved in  $\pi$ - $\pi$  and n- $\pi$  mixed excited-state configurations, attributed to intermolecular electronic coupling in organic crystals.<sup>33</sup> In addition, strong intermolecular interactions can also improve the UOP effectiveness through promoting intersystem crossing (ISC) process.<sup>34</sup> However, many of these organic molecules cannot emit fluorescence or phosphorescence in the crystal state, because of the aggregation-caused emission quenching (ACQ). The charge transfer between their excimers can quench the excitons and enhance the nonradiative transfer.<sup>35</sup>

As compared to the aggregation state phosphorescence from organic crystals, achieving ultralong single molecule phosphorescence (USMP) in dilute solutions at room temperature is even more difficult, as the triplet state of the luminescent molecule can be easily quenched by solvent molecules or air. In order to address this problem, low temperature (77K) is often utilized to slow down the molecular motion and promote the single molecule phosphorescence, which is unfavorable for practical applications.<sup>1</sup> Consequently, the development of USMP at room temperature still remains a great challenge.

Diluting organic molecules into a relatively rigid matrix can increase the effectiveness of ISC and suppress molecular motions for obtaining UOP. For example, we reported UOP from a series of molecules surrounded by polyvinyl alcohol (PVA), where strong H-bonding interactions between luminescent molecules and PVA effectively protect the triplet state of these molecules.<sup>36</sup> Recently, UOP was also obtained in an oxygen free environment by diluting dye molecules into a poly(methyl methacrylate) (PMMA) matrix with strong interactions between the host and guest molecules.<sup>37</sup> In these systems, however, the mechanisms whether the UOP is generated from a monomer or its aggregate, and how the monomer or its stacking influences the fluorescence and

phosphorescence emission are still unclear. In addition, some smart UOP materials that are responsive to water<sup>38</sup> or light<sup>39</sup> were reported, where the intermolecular interactions in these systems could be reversibly altered by the stimulus, leading to controlled photophysical properties. Therefore, it is an urgent need to reveal the relationship between stacking and emission in these systems with tunable photophysical properties.

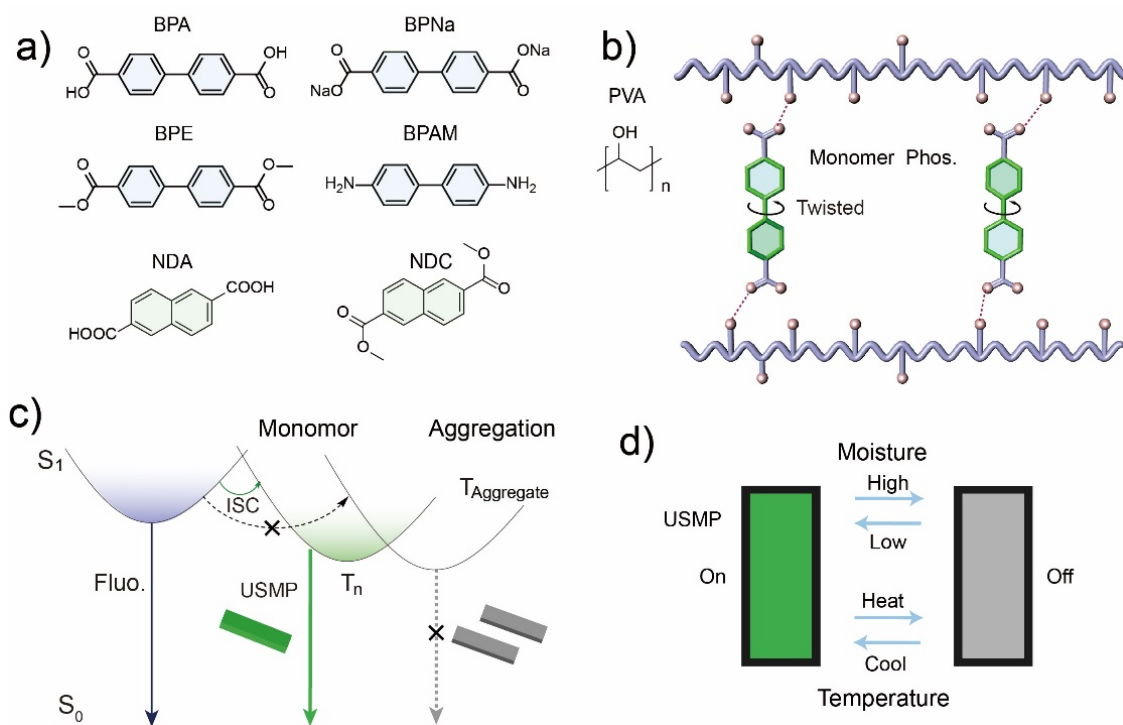


**Figure 1.** Schematic illustration of USMP and various factors that affect the USMP. (a) Chemical structures of biphenyl and naphthalene compounds. (b) Representation of coassembly. The organic molecules and PVA can form hydrogen bonds, and the organic molecules can be diluted by the PVA network. The twisted structure of the organic molecules can improve the ISC process and emit monomer phosphorescence. (c) Proposed mechanisms for USMP. The PVA networks can enhance the ISC and reduce the nonradiation transfer of the monomer exciton, enabling USMP. On the other hand, the aggregation blocks the ISC process and quenches the phosphorescence. (d)

A scheme showing reversely responsive USMP to temperature and moisture. Fluo: fluorescence, Phos: phosphorescence.

Naphthalene compounds have been found to show the room temperature phosphorescence when doped in PVA.<sup>40</sup> However, their phosphorescence lifetime is short (around 55 ms), with low phosphorescence efficiency. In addition, how the aggregation affects their phosphorescence is still unclear. More importantly, these molecules did not show responsive properties to the external stimuli. Herein, we designed to coassembly four diphenyl compounds with PVA to achieve room temperature USMP (Figure 1) and understand the basic influencing factors on USMP by using two typical naphthalene compounds as the reference. Strong intermolecular interactions between these small organic molecules and PVA matrix could significantly suppress the motions of the molecules, hence protecting their triplet state excitons.<sup>36</sup> As these small organic molecules contain O and N heteroatoms, they are also conducive to the n- $\pi$  transitions for phosphorescence<sup>41</sup> in a rigid environment (Figure 1a,b). The monomer phosphorescence emission could be proven by similar emission wavelength as compared with their dilute solution emission at 77 K. The phosphorescence lifetime of these molecules with PVA ranges from 0.3 to 0.8s, which is obviously higher than those previously reported naphthalene compounds. Powder X-ray diffraction (XRD) study confirms that the aggregation occurs in high content films. The aggregation turns off the phosphorescence but not fluorescence. The single molecule state averagely affords larger interaction energy than corresponding hydrogen bonding type dimer in PVA, suggesting that the aggregation could reduce the protection effect to these organic compounds. The aggregation depressed spin-orbit coupling

(SOC) was demonstrated by theoretical calculations. Moreover, the twist conformation is more conducive to the occurrence of ISC in molecular systems (Figure 1c), and the twisted diphenyl type compounds show higher phosphorescence emission efficiency than the naphthalene compounds with the same functional groups. Significantly, we found that the USMP from the polymer network is highly sensitive to the temperature and moisture (Figure 1d), which was not reported in previous naphthalene compounds.<sup>40</sup>

## Results and Discussion

Four organic compounds were first employed for the studies (Figure 1a), including biphenyl-4,4'-dicarboxylic acid (BPA), disodium 4,4'-biphenyldicarboxylate (BPNa), dimethyl biphenyl-4,4'-dicarboxylate (BPE), and benzidine (BPAM). UOP was observed (Figure 2a) in the coassembly films of PVA+BPA, PVA+BPNa, PVA+BPE, and PVA+BPAM by diluting 0.05 mg, 1 mg, 3 mg, 6 mg and 12 mg of each compound into 100 mg PVA, respectively. They all exhibited UOP emission at the wavelength around 500 nm, with short lifetime fluorescence from 300 to 400 nm (Figures 2b and S1). The phosphorescent lifetime for these systems was above 0.2 s (Figures 2c and S2), which corresponds to a "UOP lifetime".<sup>1</sup> In order to further confirm the emission of the coassembly films, emission spectra of the organic compounds with various concentrations in the coassemblies were investigated, where films with five ratios (0.05 mg, 1 mg, 3 mg, 6 mg, and 12 mg compounds mixed with 100 mg PVA, denoted as 005-PVA, 1-PVA, 3-PVA, 6-PVA, and 12-PVA, respectively) were prepared. In low concentrations (0.05-PVA), the organic molecules might exist in a monomer state due to the dilution effect of PVA polymer. The results show that

the phosphorescence of compound BPA dominates at low concentration coassembly films (0.05-PVA and 1-PVA), which is further enhanced up to the 6-PVA film. The fluorescence becomes more obvious in the 1-PVA film, and is enhanced with further increase of the BPA concentration (Figure 2a), accompanied with the emission color change from green to blue (Figure 2d). In the 12-PVA film, the fluorescence keeps increasing, while its phosphorescence becomes weaker.

Since BPA has a low solubility in ethanol and water, its aggregates might be formed even in the low content films. Therefore, the sodium salt (BPNa) of BPA was employed to investigate the emission at the same concentration for comparison. The monomer state of the molecule in low concentration could be achieved, as BPNa is completely soluble in water. Similar to the BPA films, strong phosphorescence with almost no fluorescence was observed in the low content film (BPNa 0.05-PVA), while the fluorescence becomes dominant at higher concentrations (Figure 2a). The BPNa 1-PVA film shows significant phosphorescence emission, since the monomer state of BPNa could still be maintained with its good solubility. For 1-PVA film of BPA, however, the fluorescence becomes extremely strong, which may be due to the emergence of BPA aggregate. For compounds BPE and BPAM, the fluorescence is dominant at all concentrations and increases more significantly than phosphorescence upon enhancing the concentrations (Figures 2a and S2). In addition, the phosphorescence from BPE and BPAM films is quite weak relative to compounds BPA and BPNa, attributed to weak intermolecular interactions between BPE (or BPAM) and PVA as compared to strong hydrogen bonding interactions between the carboxyl unit of BPA (or BPNa) and hydroxyl group of PVA. Hence, the BPA and BPNa films showed higher phosphorescence QY (Table S1) under the same coassembly concentration. Thus, we can speculate the significant

monomer phosphorescence is resulted from the strong intermolecular interactions between suitable organic molecules and PVA that protects the loaded organic molecules for emission.

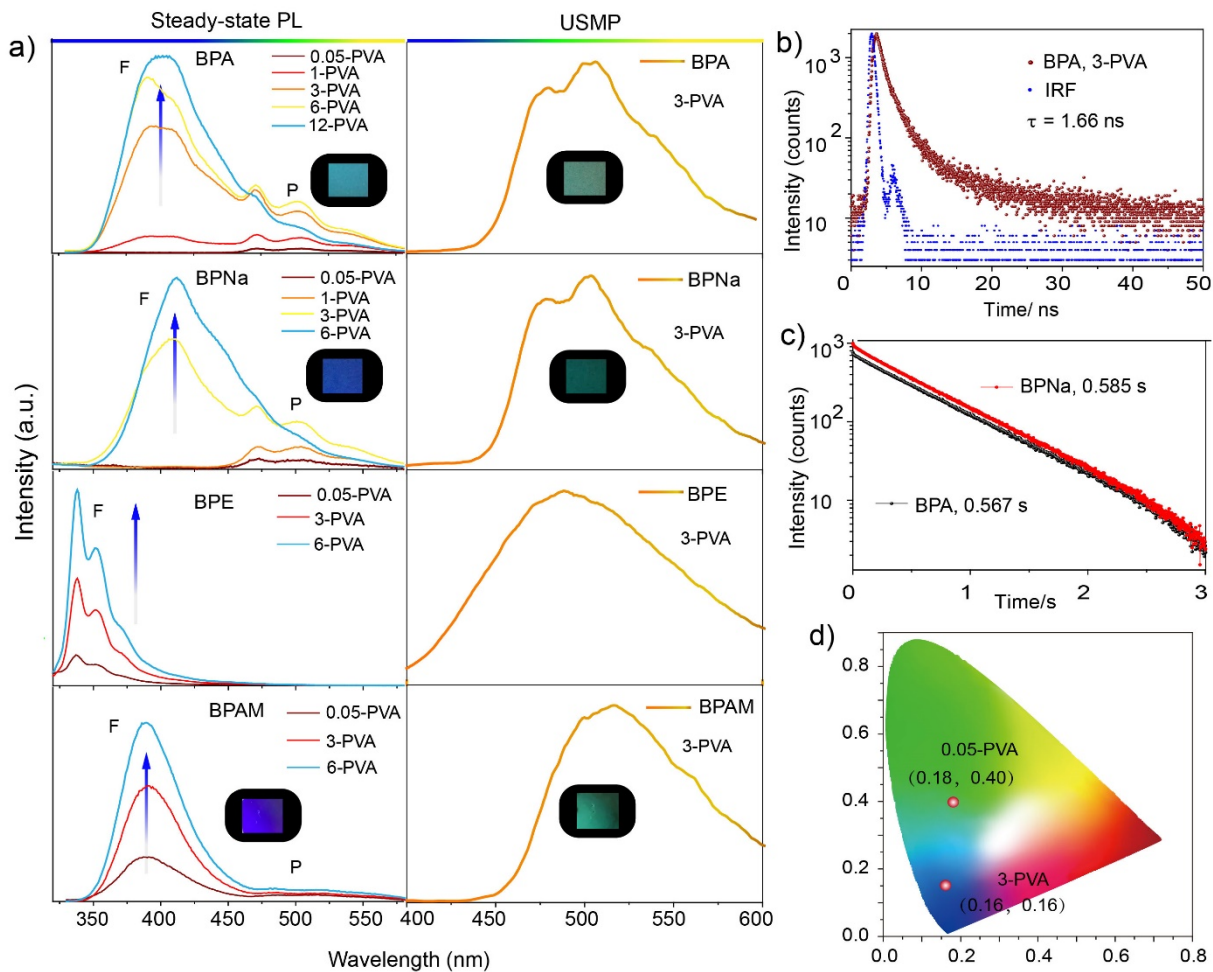


**Figure 2.** (a) Stable emission and USMP of the coassembly films consisting of BPA, BPNa, BPE and BPAM in different concentrations with PVA. Insets show photographs of BPA 1-PVA film (top images), BPNa 3-PVA film (middle images), and BPAM 3-PVA film (bottom images) under on and off of a 254 nm UV lamp under ambient conditions. (b) Fluorescence lifetime and instrument response function (IRF) of BPA 3-PVA film monitored at the emission wavelength of 400 nm ( $\lambda_{\text{ex}} = 370$  nm). (c) Phosphorescent lifetime of BPA and BPNa 3-PVA films monitored at

the emission wavelength of 500 nm ( $\lambda_{\text{ex}} = 310$  nm). (d) CIE 1931 chromaticity diagram of BPA 0.05-PVA and 3-PVA films.

The emission varies considerably with the change of the loading concentration. As discussed above, in low content films such as 0.05-PVA, the polymer might provide a dilution effect to the organic molecules in a monomer state. The varied emission feature could be due to a change from monomer to aggregate state in the coassembly system, as the aggregation is inevitable upon increasing the concentration of organic molecules.<sup>41,42</sup> In order to validate this consumption, we firstly recorded the UV-vis spectra of these systems. The coassembly films of the four compounds at low content (0.05-PVA) present a redshift as compared to their absorbance at the single molecule state in the solution (Figure S3), suggesting that there are strong intermolecular interactions between PVA and the organic molecules. However, the redshift could not confirm the monomer phosphorescence of these films. To prove the monomer phosphorescence, the emission spectra of these compounds in ethanol or methyltetrahydrofuran were measured at 77k. The maximum emission wavelength (494 nm) of the low temperature phosphorescence (Figures 3a and S4) shows a small difference to the UOP emission wavelength (501 nm) of the 3-PVA BPA film (Figures 2a and 3a), and their lifetime difference is also small (Figures 2c and S5). In addition, the peak at 463 nm in the solution state at 77k should be assigned to the vibration peak, since these molecules normally have more vibration states in low temperature. Meanwhile, we also compared the phosphorescence emission wavelength of BPAM at 77k in solution (512 nm) and 3-PVA film state (516 nm). The small wavelength difference suggests that the film phosphorescence emission is

from the monomer state (Figures 2a and S4). This is unlike many reported molecules showing a large redshift when comparing their aggregate state phosphorescence wavelength to the monomer phosphorescence wavelength.<sup>1</sup> As a result, the UOP emission in the present films originates from the monomer phosphorescence. The strong intermolecular interactions between the organic molecules and PVA could greatly restrict non-radiative transfer and facilitate the triplet emission of the monomer. For high content films of BPA-PVA (Figure 3b) and BPAM-PVA (Figure S6), their largest absorbance wavelength did not show any significant change upon increasing the concentration. On the other hand, the largest absorbance wavelength shows an obvious blue shift for both BPNa-PVA (Figure 3c) and BPE-PVA (Figure S6) when increasing the concentration of the organic molecules, suggesting the restriction by the *H*-aggregation formation of BPNa and BPE in high content films.<sup>43-46</sup>

To better understand how the aggregation state influences the phosphorescence emission, wide angle X-ray scattering (WAXS) was employed to detect the stacking parameters of the films. Since conventional XRD technology is difficult to detect the diffraction signals of polymer films, we used the X-ray scattering technique to study the film samples. The pure PVA film shows two scattering peaks at  $q = 1.37 \text{ \AA}^{-1}$  ( $2\theta = 19.23^\circ$ ) and  $2.81 \text{ \AA}^{-1}$  ( $2\theta = 40.31^\circ$ ), and the BPA 0.05-PVA film presents similar scattering peaks, suggesting that the organic molecule in PVA remains in its monomer state (Figure 3d). However, no significant scattering peak was found in the BPA 1-PVA film, probably because of the transition state under this ratio. Interestingly, two new major scattering peaks at  $q = 0.43 \text{ \AA}^{-1}$  and  $0.81 \text{ \AA}^{-1}$  were observed from BPA 3-PVA film, along with two weak scattering peaks at  $q = 1.77 \text{ \AA}^{-1}$  and  $1.87 \text{ \AA}^{-1}$ . The scattering peaks at  $q = 1.77 \text{ \AA}^{-1}$  (with the

distance of 3.55 Å) and 1.87 Å<sup>-1</sup> (with the distance of 3.36 Å) become more obvious in the case of BPA 6-PVA film (Figures 3d,e and S7), which should be related to the  $\pi$ - $\pi$  stacking interaction (3~4 Å) of the organic molecule for the formations of dimers, trimers or higher oligomers. Thus, the luminescent property of these coassembly films is unavoidably influenced by the stacking effect (Figures S8 and S9). Furthermore, transmission electronic microscopy (TEM) was employed to study the coassembly process. Similar to previous reports,<sup>36</sup> an even grid-like distribution of nanowires was found at low content 0.05-PVA films (Figure S10a,d), confirming that no aggregation was formed under this concentration. When 1 mg and 3 mg BPA were loaded into PVA, larger block aggregates were observed (Figure S10b,c). Compound BPNa also exhibited a similar trend (Figure S10d-f), supporting the WAXS results.

To gain further understanding of the stacking effect among the aggregated molecules, single crystal structures of BPA,<sup>47</sup> BPAM,<sup>48</sup> BPNa and BPE were obtained and analyzed. The crystal structures indicate that all four compounds exhibit  $\pi$ - $\pi$  stacking interactions (Figures 3f and S11), agreeing well with the WAXS results. Thus, these molecules at high concentration in the films should have a similar stacking mode as the crystal state. The  $\pi$ - $\pi$  stacking based dimers in high coassembly concentration would unavoidably change the luminescent property of the compounds as compared to the monomer state in low concentration. In addition, hydrogen-bonded dimers (Figure S12) were also observed in the crystal state, due to the interaction of carboxyl groups. This could be another important stacking mode at high concentration, attributing to the increased two-dimensional extension of the films.

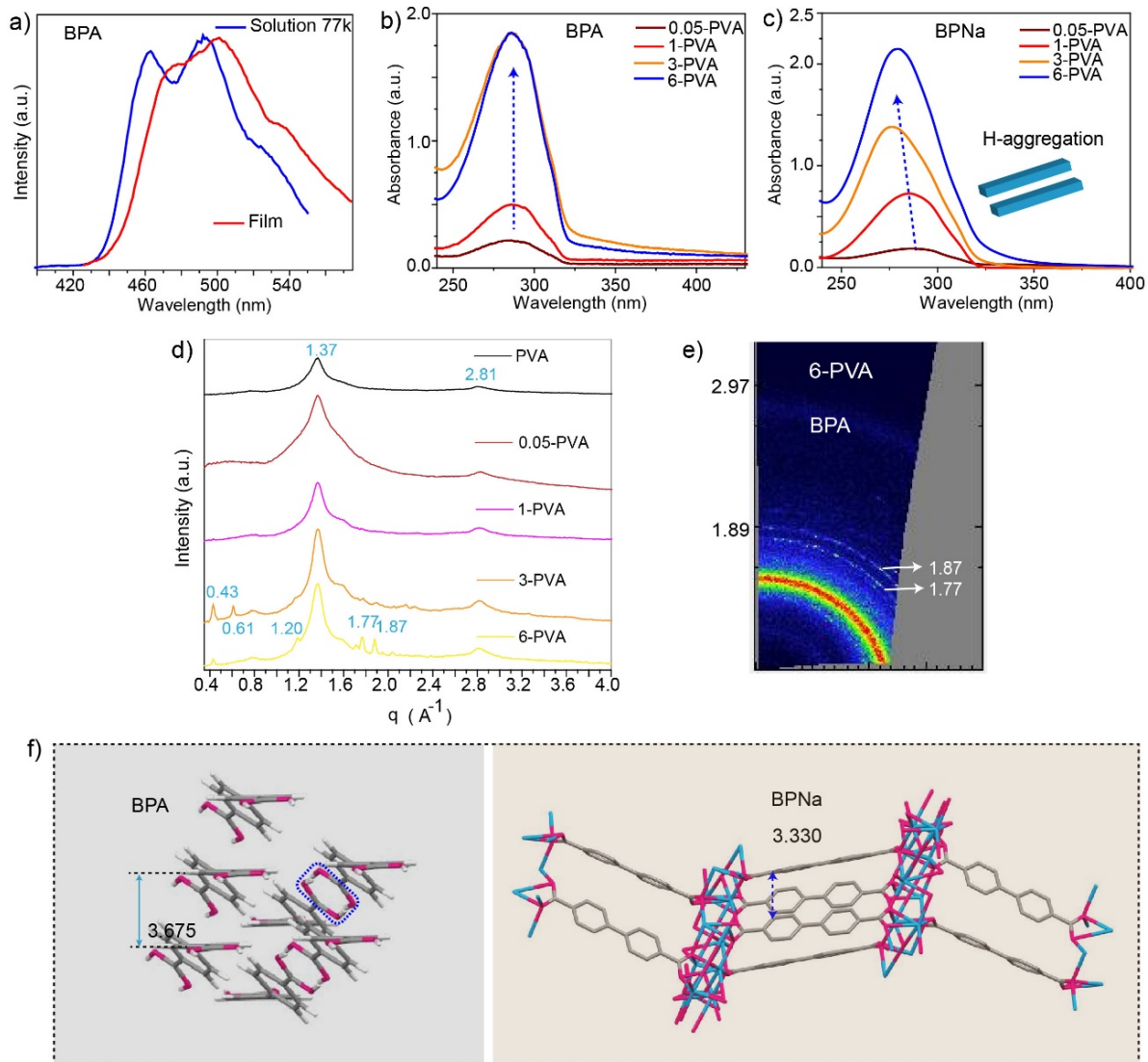


**Figure 3.** (a) Phosphorescence spectra of BPA in ethanol ( $10\ \mu\text{M}$ ) at 77k and in film (3-PVA) at room temperature under 290 nm excitation. (b,c) Absorbance of BPA and BPNa in different coassembly concentrations with PVA. (d) WAXS patterns of PVA loaded with BPA at different concentration. (e) WAXS photograph of 6-PVA loaded with BPA. (f) Dimer structures observed from the single crystals of BPA and BPNa.

Knowing that the stacking effect has a significant influence on the emission of the systems, we then investigated the emission of the aggregation state using powders and crystals. No phosphorescence was observed in powders and crystals of the compounds even at low temperature of 77 K (Figures 4a,b, S13, and S14). Instead, fluorescence was observed, where the emission in the powder state of BPNa, BPE and BPAM was stronger than that in the crystal state (Figures 4b and S13). From the powder XRD studies (Figures 4c and S15), the  $\pi$ - $\pi$  stacking interaction is also obvious in the powder state, proving that the powder has the similar aggregation mode to the single crystal. Thus, it was suggested that the phosphorescence is quenched by the stacking, while moderate stacking is useful to the fluorescence generation. In addition, higher content coassembly films show higher quantum yield (QY) than that of lower content films. Powders exhibit the highest QY (Table S1) on account of the enhanced fluorescence, indicating the reduced ISC efficiency under the aggregation. The moderate stacking could restrict molecular motions and thus reduce the nonradiative transition together with less harmful aggregation effect on the fluorescence efficiency.<sup>49</sup> From these observations and previous spectral studies of films, powders and crystals, it was concluded that the stacking quenches the phosphorescence on the coassembly state even when the aggregated molecules have the same environment with the monomer ones. The ISC process would be depressed by the aggregation in these molecular systems. It should be noticed that the high content films (3-PVA film and 6-PVA film) also showed strong phosphorescence. In this case, while PVA is dominant in these films, many organic molecules still keep their monomer state within PVA. On the other hand, other organic molecules at the aggregate state would induce the fluorescence emission.

A series of theoretical calculations were conducted to obtain further insights for that the phosphorescence is more readily achieved in the monomer state than in the aggregate state of these biphenyl compounds. Quantum-chemical modelling was utilized to investigate this phenomenon from the organization of the  $S_1$  and low-lying  $T_n$  states, the SOC efficiency between these states, and their radiative lifetimes. As shown from Figure 4d, the SOC matrix element (SOCME) between the  $S_1$  and  $T_3$  excited states for the monomer of compound BPA is very large ( $7.28 \text{ cm}^{-1}$ ), which conveys very fast  $S_1$ - $T_3$  ISC and subsequent efficient population of the  $T_1$  state through the spin-allowed  $T_3$ - $T_1$  internal conversion. A clear increase of SOCME between the  $S_1$  and  $T_1$  states with the rise of twist angle between the two benzene rings of BPA (Figure S16) was observed, suggesting that the distorted conformation is conducive to the ISC.<sup>50,51</sup> Thus, it was proposed that, in the absence of aggregates, an efficient  $S_1$ - $T_3$ - $T_1$  deactivation pathway is the main reason behind the observation of the dominant phosphorescence emission at low BPA content in the PVA matrix. The calculated radiative lifetime of the  $T_1$  state was about 0.2 s, which is close to the experimental measurement (about 0.56 s). H-bonded and  $\pi$ -stacked dimers taken from the single crystal structure were considered here for the estimation of aggregation effect on the phosphorescence rate. It was found that the efficiency of the  $S_1$ - $T_n$  ISC channels becomes smaller (*i.e.*, SOCME is much smaller as compared with  $S_1$ - $T_3$  in the single molecule) and the average radiation lifetime ( $\tau_{av}$ ) of  $T_1$  state becomes longer (1.15 and 2.53 s for H-bonded and  $\pi$ -stacked dimers, respectively) than that of the monomer. Meanwhile, quantitative interaction energy of PVA fragments with single molecule BPA and its hydrogen bonding type dimer was calculated for investigating the strength of molecular interaction (Figure 4e). It was found that each BPA molecule in the single molecule state

averagely obtains larger interaction energy than the dimer state, suggesting that PVA has better protection effect to the single molecule BPA than hydrogen bonding type dimer. The formation of hydrogen bonding type dimer may cause more nonradiation transfer to quench the phosphorescence than single molecule BPA in PVA. Thus, these factors are related to the occurrence of phosphorescence. These results agree well with the fact that the phosphorescence is almost impossible in the aggregate state.

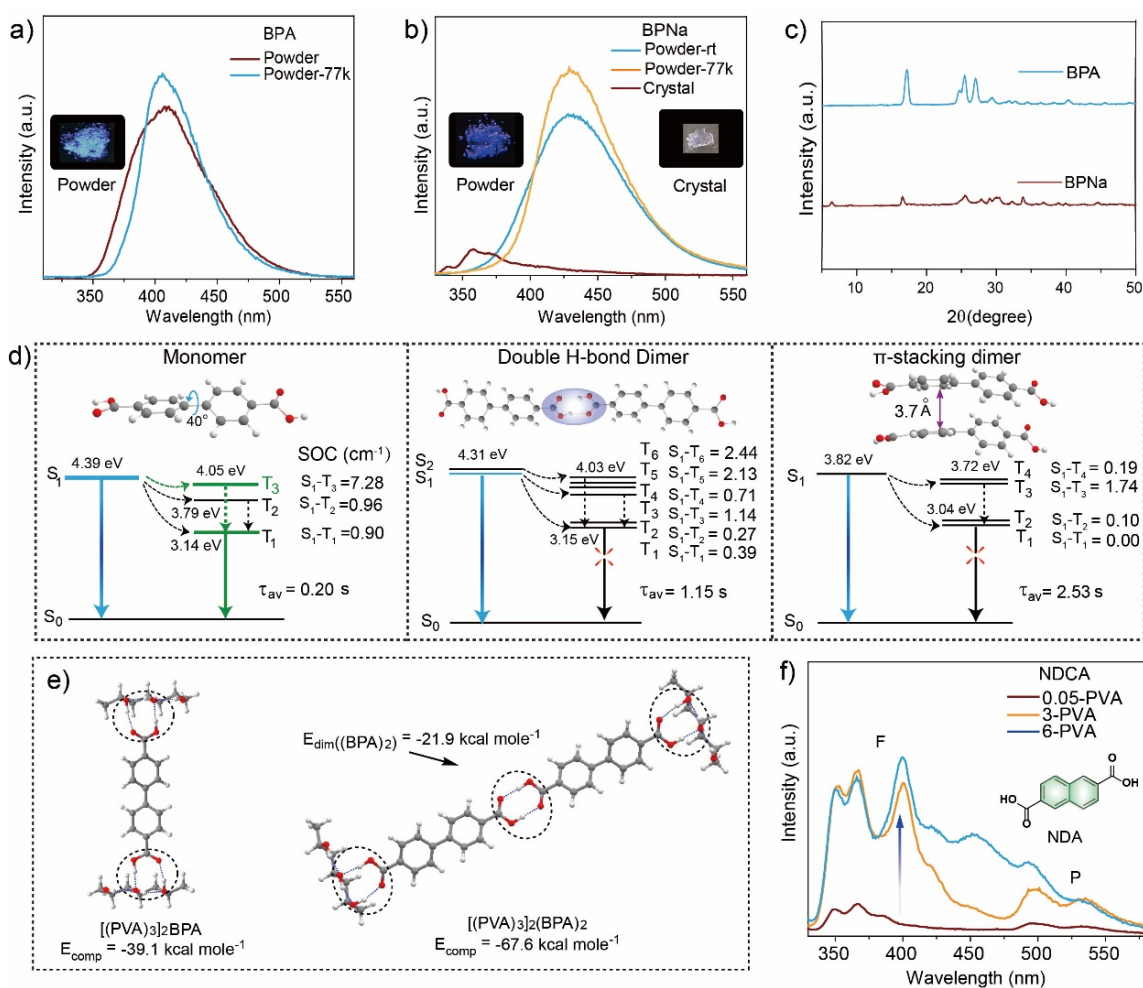


**Figure 4.** (a) Emission spectra of BPA in the powder state at 77k and room temperature ( $\lambda_{ex} = 310$  nm). (b) Emission spectra of BPNa in the powder state at 77k and room temperature, and in the crystal state at room temperature ( $\lambda_{ex} = 310$  nm). (c) Powder XRD spectra of BPNa and BPA in the

powder state. (d) Diagrams of molecular energy levels for the single molecule (left), hydrogen-bonded dimer (middle) and  $\pi$ - $\pi$  stacking dimer (right) of BPA. Solid and dashed arrows denote the radiative and nonradiative transitions, respectively. Blue and green lines correspond to the fluorescence and phosphorescence pathways, respectively. (e) Interaction energy for the optimized complexes of PVA fragments with BPA single molecule and its hydrogen bonding type dimer. (f) Stable emission spectra of NDA-based PVA films at different NDA concentrations.  $\tau_{\text{av}}$ : The average radiation lifetime of  $T_1$  state.

Similar to compound BPA, the USMP of sodium-containing compound BPNa in the PVA matrix at room temperature (Figure S17) is induced by a quite strong SOC between  $S_1$  and  $T_1$  states (SOCME =  $1 \text{ cm}^{-1}$ ) together with a small  $S_1$ - $T_1$  gap (0.12 eV). The simulations predict that USMP in BPE-loaded PVA is caused by the  $S_1$ - $T_4$  ISC for the population of the  $T_1$  state through  $T_4$ - $T_1$  internal conversion (Figure S18). However, the SOC becomes very small in the dimer state of BPE, and the USMP is completely quenched by the aggregation. BPAM demonstrates USMP through the  $S_1$ - $T_3$ - $T_1$  channel (Figure S19), while small SOC and large radiative lifetime ( $>100 \text{ s}$ ) for the  $T_1$  state in the dimer of BPMA suggest that the phosphorescence is difficult to occur in the aggregate state (Figure S19c). Similar to BPA, BPAM in the single molecule state also averagely obtains larger interaction energy than its dimer state (Figure S19d). Thus, these calculated results well explain that the ISC process is efficient in the monomer state, while it is reduced by the aggregation in these systems. Twisted conformation of compound BPAM also demonstrates more efficient USMP emission than the planar conformation through the  $S_1$ - $T_3$ - $T_1$  channel (Figure S19).

This is in line with Minaev's analysis that breaking the planarity of conjugated systems induces the  $\sigma$ - $\pi$  mixing of corresponding molecular orbital and promotes comparatively large SOC between corresponding electronic states, leading to enhanced ISC and phosphorescence.<sup>52,53</sup> While moderately twisted conformation is beneficial to the ISC process, we also know that excessive distortion could cause excessive molecular motion that would enhance the nonradiative decay. It was noticed that compound BPA is also moderately twisted, which would be conducive to the phosphorescence emission. Because BPE has more planar conformation, we could understand why it shows very weak USMP emission (Figure 2a). In addition, strong intermolecular interactions such as hydrogen bonding interactions between the dye molecules and PVA network could also induce the distortion of the dye molecules, because the dye molecules need to cater to the polymer network. Naturally, the molecules with carboxyl groups show higher emission than those having ester and amino groups.

The above phenomenon was not just discovered from diphenyl compounds, but also from some naphthalene compounds (Figure 1a) including 2,6-naphthalenedicarboxylic acid (NDA) and dimethyl 2,6-naphthalenedicarboxylate (NDE). NDA and NDE in the PVA matrix also show a similar emission phenomenon as the diphenyl compounds (Figures 4f and S20-S22). Since NDA and NDE have more planar conformation than the biphenyl compounds, they showed lower phosphorescence QY (Table S1). USMP and the aggregation-quenched phosphorescence were observed in these systems (Figures 4f and S20-S24). Their phosphorescence lifetime is higher than previously reported naphthalene molecules,<sup>40</sup> because they have more functional groups to induce stronger intermolecular interactions. Moreover, the fluorescence was continuously enhanced in the

coassembly system upon increasing the content of NDA (Figure 4f) or NDE (Figure S21). Their powders exhibit strong fluorescence as well (Figures S20-S22 and Table S1). Stronger and redshifted fluorescence emission (around 450 nm) of the PVA films with higher NDA contents as compared to lower concentration ones may be due to the formation of *J*-type aggregates.

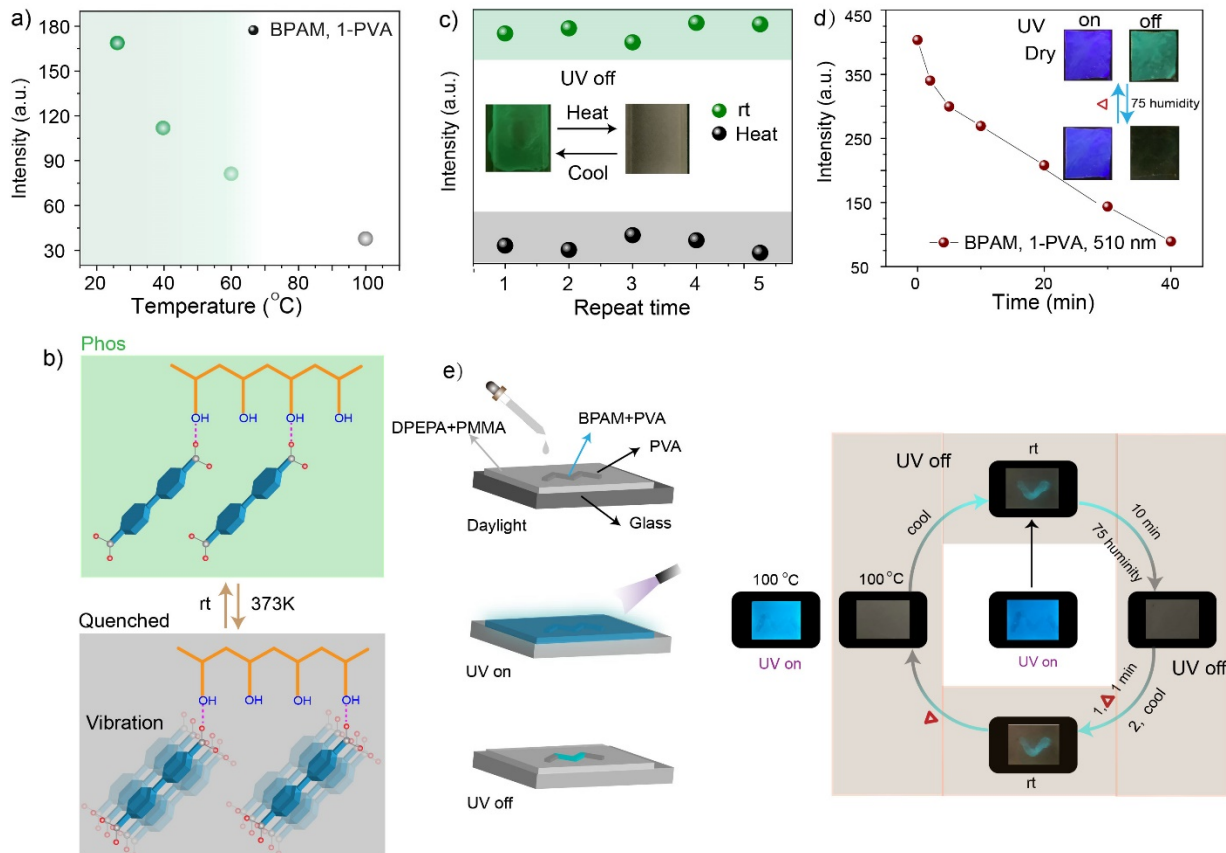


**Figure 5.** Moisture and temperature responsible anti-counterfeiting. (a) Emission intensity changes of BPAM-based 1-PVA film at 510 nm under different temperatures. (b) Schematic mechanism for high temperature induced vibration quenching of the USMP emission. (c) Emission intensity changes of BPAM-based 1-PVA film at 510 nm by alternatively changing the temperature between 373 k and room temperature over five cycles. (d) Emission intensity changes of BPAM-based 1-PVA film at 510 nm in 75% humidity environment over time. (e) Fabrication process of the film

for security protection (left diagram), and photographs of the obtained film under different conditions (right diagram). rt: room temperature.

Having demonstrated USMP in the coassembly systems, we subsequently studied their distinct properties as compared to crystalline materials for UOP. Firstly, we found that the coassembly films were highly sensitive to temperature variations. At higher temperature such as 373K, the USMP intensity of the coassembly films was extremely lower than its intensity at room temperature (Figures 5a and S25). The phosphorescence of the coassembly systems showed more sensitive response to the temperature as compared to corresponding crystals probably because that the closed stacking in crystals blocks the excitons.<sup>54</sup> High temperature could easily destroy the crystal structure and change the luminescent properties, making the reversible response to the temperature impossible.<sup>1,54</sup> The enhanced molecular vibration and rotation at high temperature trigger the non-radiative decay to suppress the phosphorescence emission (Figure 5b). Interestingly, the monomer state within thin and flexible films made the phosphorescence highly sensitive to temperature. The materials could be reversibly restored to the original state that emits strong phosphorescence at room temperature. Such a reversible process could be cycled at least five times (Figure 5c) of 1-PVA film of BPAM.

Secondly, the coassembly films were also highly sensitive to the humidity of air. The BPAM-PVA films were chosen as a presentative example for studying the moisture-responsive process. Figure 5d presents the change of the emission intensity at the wavelength of 510 nm. In 75% moisture environment, the emission intensity decreased to the level about 5 times less than the

initial stage within 40 min. The photographs in Figure 5d show that the USMP of BPAM-based 1-PVA film almost vanishes under the UV light in 75% moisture environment for 40 min. The quenching of the USMP emission could be due to the weakening and breaking of the intermolecular hydrogen bond network between the PVA host and BPAM molecule by water interference (Figure S26). Fourier-transform infrared spectroscopy (Figure S26b) exhibits that the deformation N-H vibration at  $1650\text{ cm}^{-1}$  obviously decreases, indicating that the hydrogen bonding between the amino group and PVA is interrupted by water molecule in air.

The fact that the coassembly films could distinctly respond to the temperature and moisture brings about promising applications in the security protection field, such as information storage, encryption, and anti-counterfeiting. Therefore, a smart security protection technology using BPAM-based 1-PVA film and blue emitting planar diphenyl-diacetylene molecule (DPEPA)<sup>49</sup> was developed in 50% humidity. The fabrication process is shown in Figure 5e. First, the character “V” is written by a dropper using BPAM-based 1-PVA solution and dried at  $80\text{ }^{\circ}\text{C}$  for 20 min. Second, another “V” is written to obtain the character “W” by pure PVA solution followed by drying. Third, the information is covered by a DPEPA-PMMA film with drying. The “W” pattern was visible under daylight on account of the phase separation of the PVA and PMMA films. No pattern was observed upon exposure to the 254 nm UV lamp because of the masking by strong emission of the DPEPA-PMMA cover film. Interestingly, the pattern “V” became visible for several seconds after the removal of the UV light, attributed to the existence of the USMP emission. When putting the film in 75% humidity condition for 20 min, the “V” pattern vanished after turning off the UV light, because the interaction with sufficient water molecule quenched the USMP emission.

The pattern “V” could be restored by simply heating the film at 100 °C for 2 min and then cooling it down to room temperature. Furthermore, the pattern “V” disappeared upon heating the film to 100 °C for 5 min, since high temperature induced vibrations could quench the USMP emission. The USMP emission was restored when cooling the film to the room temperature. It should be noted that the fluorescence did not show any obvious change during this process, proving that the USMP is much more sensitive to temperature than fluorescence. Hence, this operation indicates that smartly and reversibly switching the USMP emission by moisture and temperature could be used for the information encryption and decryption. As compared with conventional crystal based UOP materials having low stability at high temperature and poor processability, the present film is more stable, flexible, and easy to process. These remarkable advantages make these films highly promising for anti-counterfeiting and security applications.

## **Conclusions**

In this work, we have conducted a thorough research by achieving ultralong single molecule phosphorescence within PVA polymer matrix, and studied how the aggregation, conformation, temperature, and moisture could influence the monomer phosphorescence. The USMP was obtained by forming supramolecular networks between these small organic molecules and PVA, and confirmed by several techniques including photophysical spectra and powder XRD studies. The aggregation of the dye molecules within the polymer matrix was investigated by WAXS technology, where obvious stacking similar to the solid state was observed in these coassembly systems. By combining the emission spectral studies of film, powder and crystal states, it was

concluded that the ultralong monomer phosphorescence is turned off when the aggregation of these small organic molecules is formed even in the PVA matrix. More interestingly, the aggregation could permit the fluorescence, suggesting that the ISC process is blocked in the aggregation state. The theoretical calculations proved that the aggregation quenched phosphorescence was due to a depressed SOC between the excited singlet and triplet states, and PVA had better protection effect to the single molecule than hydrogen bonding type dimer. Due to the twisted conformation, these diphenyl compounds showed higher phosphorescence emission efficiency than the naphthalene compounds with the same functional group. Moreover, the USMP could also be depressed upon changing the temperature or humidity. Significantly, the USMP could be switched reversibly in the supramolecular networks by responding to the changes of temperature and humidity. The temperature- and humidity-responsive films were utilized as smart materials for important anti-counterfeiting and security applications. The flexible, reversible and robust nature of the films is preferable over conventional crystal based UOP materials in these applications. Therefore, the present research not only demonstrates the monomer phosphorescence, but also might open an avenue for developing smart fluorescence and phosphorescence systems toward practical applications.

## **Experimental Section**

**Preparation of coassembly films.** PVA-100 (5g) was added in deionized water (500 mL), which was stirred in 100 °C for 1 h. Small organic molecules with same concentrations but different volumes (0.05 mg/0.05 mL, 1 mg/1mL, 3 mg/3 mL, 6 mg/6 mL and 12 mg/12 mL) were added

into the prepared PVA solution (10 mL). The obtained solutions were then ultrasonicated at 60 °C for 20 min to complete the coassembly. Dropping the solutions (about 0.5 mL) on quartz glass and keeping it at 80 °C for 3 h resulted in the coassembly films.

**Supporting Information.** The Supporting Information is available free of charge on the ACS Publications website at DOI

Synthesis, characterization and computation details, fluorescence and phosphorescent spectra and lifetime, absorbance spectra, WAXS patterns, TEM images, single crystal structures, powder XRD patterns, quantum yields, diagrams of molecular energy levels, natural transition orbital pairs, NMR spectra, and movie S1 for temperature-responsive phosphorescence.

Crystal CIF files for BPE and BPNa.

## **AUTHOR INFORMATION**

### **Corresponding Author**

Email: zhaoyanli@ntu.edu.sg; hagren@kth.se.

**Acknowledgement.** This research is supported by the Singapore Agency for Science, Technology and Research (A\*STAR) AME IRG grant (No. A1883c0005), and the Singapore National Research Foundation Investigatorship (No. NRF-NRFI2018-03).

## **References**

(1) Xu, S.; Chen, R.; Zheng, C.; Huang, W. Excited State Modulation for Organic Afterglow:

Materials and Applications. *Adv. Mater.* **2016**, *28*, 9920–9940.

(2) Cai, S. Z.; Shi, H.; Li, J.; Gu, L.; Ni, Y.; Cheng, Z.; Wang, S.; Xiong, W.-W.; Li, L.; An, Z.; Huang, W. Visible-Light-Excited Ultralong Organic Phosphorescence by Manipulating Intermolecular Interactions. *Adv. Mater.* **2017**, *29*, 1701244.

(3) Zhao, W.; Cheung, T. S.; Jiang, N.; Huang, W.; Lam, J. W. Y.; Zhang, X.; He, Z.; Tang, B. Z. Boosting the Efficiency of Organic Persistent Room-Temperature Phosphorescence by Intramolecular Triplet-Triplet Energy Transfer. *Nat. Commun.* **2019**, *10*, 1595.

(4) He, Z.; Zhao, W.; Lam, J. W. Y.; Peng, Q.; Ma, H.; Liang, G.; Shuai, Z.; Tang, B. Z. White Light Emission from a Single Organic Molecule with Dual Phosphorescence at Room Temperature. *Nat. Commun.* **2017**, *8*, 416.

(5) Fateminia, S. A.; Mao, Z.; Xu, S.; Yang, Z.; Chi, Z.; Liu, B. Organic Nanocrystals with Bright Red Persistent Room-Temperature Phosphorescence for Biological Applications. *Angew. Chem. Int. Ed.* **2017**, *56*, 12160-12164.

(6) Kwon, M. S.; Lee, D.; Seo, S.; Jung, J.; Kim, J. Tailoring Intermolecular Interactions for Efficient Room-Temperature Phosphorescence from Purely Organic Materials in Amorphous Polymer Matrices. *Angew. Chem. Int. Ed.* **2014**, *53*, 11177-11181.

(7) Gong, Y.; Zhao, L.; Peng, Q.; Fan, D.; Yuan, W. Z.; Zhang, Y.; Tang, B. Z. Crystallization-Induced Dual Emission from Metal- and Heavy Atom-Free Aromatic Acids and Esters. *Chem. Sci.* **2015**, *6*, 4438-4444.

(8) Gong, Y.; Chen, G.; Peng, Q.; Yuan, W. Z.; Xie, Y.; Li, S.; Zhang, Y.; Tang, B. Z. Achieving Persistent Room Temperature Phosphorescence and Remarkable Mechanochromism from Pure

Organic Luminogens. *Adv. Mater.* **2015**, *27*, 6195-6201.

(9) Chen, H.; Ma, X.; Wu, S.; Tian, H. A Rapidly Self-Healing Supramolecular Polymer Hydrogel with Photostimulated Room-Temperature Phosphorescence Responsiveness. *Angew. Chem. Int. Ed.* **2014**, *53*, 14149-14152.

(10) Kabe, R.; Adachi, C. Organic Long Persistent Luminescence. *Nature* **2017**, *550*, 384-387.

(11) Su, Y.; Phua, S. Z. F.; Li, Y.; Zhou, X.; Jana, D.; Liu, G.; Lim, W. Q.; Ong, W. K.; Yang, C.; Zhao, Y. L. Ultralong Room Temperature Phosphorescence from Amorphous Organic Materials toward Confidential Information Encryption and Decryption. *Sci. Adv.* **2018**, *4*, eaas9732.

(12) Chen, X.; Xu, C.; Wang, T.; Zhou, C.; Du, J.; Wang, Z.; Xu, H.; Xie, T.; Bi, G.; Jiang, J.; Zhang, X.; Demas, J.; Trindle, C.; Luo, Y.; Zhang, G. Versatile Room-Temperature-Phosphorescent Materials Prepared from *N*-Substituted Naphthalimides: Emission Enhancement and Chemical Conjugation. *Angew. Chem. Int. Ed.* **2016**, *55*, 9872-9876.

(13) Jiang, K.; Zhang, L.; Lu, J.; Xu, C.; Cai, C.; Lin, H. Triple-Mode Emission of Carbon Dots: Applications for Advanced Anti-Counterfeiting. *Angew. Chem. Int. Ed.* **2016**, *55*, 7231-7235.

(14) Cai, S.; Ma, H.; Shi, H.; Wang, H.; Wang, X.; Xiao, L.; Ye, W.; Huang, K.; Cao, X.; Gan, N.; Ma, C.; Gu, M.; Song, L.; Xu, H.; Tao, Y.; Zhang, C.; Yao, W.; An, Z.; Huang, W. Enabling Long-Lived Organic Room Temperature Phosphorescence in Polymers by Subunit Interlocking. *Nat. Commun.* **2019**, *10*, 4247.

(15) Ma, X.; Xu, C.; Wang, J.; Tian, H. Amorphous Pure Organic Polymers for Heavy-Atom-Free Efficient Room-Temperature Phosphorescence Emission. *Angew. Chem. Int. Ed.* **2018**, *57*, 10854-10858.

- (16) Chen, H.; Yao, X.; Ma, X.; Tian, H. Amorphous, Efficient, Room-Temperature Phosphorescent Metal-Free Polymers and Their Applications as Encryption Ink. *Adv. Opt. Mater.* **2016**, *4*, 1397-1401.
- (17) Ma, X.; Wang, J.; Tian, H. Assembling-Induced Emission: An Efficient Approach for Amorphous Metal-Free Organic Emitting Materials with Room-Temperature Phosphorescence. *Acc. Chem. Res.* **2019**, *52*, 738-748.
- (18) Zhao, W.; He, Z.; Lam, J. W. Y.; Peng, Q.; Ma, H.; Shuai, Z.; Bai, G.; Hao, J.; Tang, B. Z. Rational Molecular Design for Achieving Persistent and Efficient Pure Organic Room-Temperature Phosphorescence. *Chem* **2016**, *1*, 592-602.
- (19) Huang, L.; Chen, B.; Zhang, X.; Trindle, C. O.; Liao, F.; Wang, Y.; Miao, H.; Luo, Y.; Zhang, G. Proton-Activated “Off-On” Room-Temperature Phosphorescence from Purely Organic Thioethers. *Angew. Chem. Int. Ed.* **2018**, *57*, 16046-16050.
- (20) Shi, H.; Ye, W.; Yao, X.; Wang, Q.; Dong, C.; Jia, W.; Ma, H.; Cai, S.; Huang, K.; Fu, L.; Zhang, Y.; Zhi, J.; Gu, L.; Zhao, Y.; An, Z.; Huang, W. Amorphous Ionic Polymers with Color-Tunable Ultralong Organic Phosphorescence. *Angew. Chem. Int. Ed.* **2019**, *58*, 18776-18782.
- (21) Yang, Z.; Mao, Z.; Zhang, X.; Ou, D.; Mu, Y.; Zhang, Zhao, C.; Liu, S.; Chi, Z.; Xu, J.; Wu, C.; Lu, P.; Lien, A.; Bryce, M. Intermolecular Electronic Coupling of Organic Units for Efficient Persistent Room-Temperature Phosphorescence. *Angew. Chem. Int. Ed.* **2016**, *55*, 2181-2185.
- (22) Wang, X. F.; Xiao, H.; Chen, P. Z.; Yang, Q. Z.; Chen, B.; Tung, C. H.; Chen, Y.; Wu, L. Z. Pure Organic Room Temperature Phosphorescence from Excited Dimers in Self-Assembled Nanoparticles under Visible and Near-Infrared Irradiation in Water. *J. Am. Chem. Soc.* **2019**, *141*,

5045–5050.

(23) Xie, Y.; Ge, Y.; Peng, Q.; Li, C.; Li, Q.; Li, Z. How the Molecular Packing Affects the Room Temperature Phosphorescence in Pure Organic Compounds: Ingenious Molecular Design, Detailed Crystal Analysis, and Rational Theoretical Calculations. *Adv. Mater.* **2017**, *29*, 1606829.

(24) Zhang, X.; Xie, T.; Cui, M.; Yang, L.; Sun, X.; Jiang, J.; Zhang, G. General Design Strategy for Aromatic Ketone-Based Single-Component Dual-Emissive Materials. *ACS Appl. Mater. Interfaces* **2014**, *6*, 2279-2284.

(25) Yang, X.; Yan, D. Strongly Enhanced Long-Lived Persistent Room Temperature Phosphorescence Based on the Formation of Metal-Organic Hybrids. *Adv. Opt. Mater.* **2016**, *4*, 897-905.

(26) Mu, Y.; Yang, Z.; Chen, J.; Yang, Z.; Li, W.; Tan, X.; Mao, Z.; Yu, T.; Zhao, J.; Zheng, S.; Liu, S.; Zhang, Y.; Chi, Z.; Xu, J.; Aldred, M. P. Mechano-Induced Persistent Room-Temperature Phosphorescence from Purely Organic Molecules. *Chem. Sci.* **2018**, *9*, 3782-3787.

(27) Yang, J.; Zhen, X.; Wang, B.; Gao, X.; Ren, Z.; Wang, J.; Xie, Y.; Li, J.; Peng, Q.; Pu, K.; Li, Z. The Influence of the Molecular Packing on the Room Temperature Phosphorescence of Purely Organic Luminogens. *Nat. Commun.* **2018**, *9*, 840.

(28) Lucenti, E.; Forni, A.; Botta, C.; Carlucci, L.; Giannini, C.; Marinotto, D.; Pavanello, A.; Previtali, A.; Righetto, S.; Cariati, E. Cyclic Triimidazole Derivatives: Intriguing Examples of Multiple Emissions and Ultralong Phosphorescence at Room Temperature. *Angew. Chem. Int. Ed.* **2017**, *56*, 16302-16307.

- (29) He, Z.; Gao, H.; Zhang, S.; Zheng, S.; Wang, Y.; Zhao, Z.; Ding, D.; Yang, B.; Zhang, Y.; Yuan, W. Z. Achieving Persistent, Efficient, and Robust Room-Temperature Phosphorescence from Pure Organics for Versatile Applications. *Adv. Mater.* **2019**, *31*, 1807222.
- (30) Chen, J.; Yu, T.; Ubba, E.; Xie, Z.; Yang, Z.; Zhang, Y.; Chi, Z. Achieving Dual-Emissive and Time-Dependent Evolutive Organic Afterglow by Bridging Molecules with Weak Intermolecular Hydrogen Bonding. *Adv. Opt. Mater.* **2019**, *7*, 1801593.
- (31) Zhou, Y.; Yin, L.; Hang, C.; Li, X.; Ågren, H.; Yi, T.; Zhang, Q.; Zhu, L. Helical Self-Assembly-Induced Singlet-Triplet Emissive Switching in a Mechanically Sensitive System. *J. Am. Chem. Soc.* **2017**, *139*, 785-791.
- (32) An, Z.; Zheng, C.; Tao, Y.; Chen, R.; Shi, H.; Chen, T.; Wang, Z.; Li, H.; Deng, R.; Liu, X.; Huang, W. Stabilizing Triplet Excited States for Ultralong Organic Phosphorescence. *Nat. Mater.* **2015**, *14*, 685-690.
- (33) Yang, J.; Ren, Z.; Xie, Z.; Liu, Y.; Wang, C.; Xie, Y.; Peng, Q.; Xu, B.; Tian, W.; Zhang, F.; Chi, Z.; Li, Q.; Li, Z. AIEgen with Fluorescence-Phosphorescence Dual Mechanoluminescence at Room Temperature. *Angew. Chem. Int. Ed.* **2017**, *56*, 880-884.
- (34) Zhou, B.; Yan, D. Hydrogen-Bonded Two-Component Ionic Crystals Showing Enhanced Long-Lived Room-Temperature Phosphorescence via TADF-Assisted Förster Resonance Energy Transfer. *Adv. Funct. Mater.* **2019**, *29*, 1807599.
- (35) Hong, Y.; Lam, J. W. Y.; Tang, B. Z. Aggregation-Induced Emission. *Chem. Soc. Rev.* **2011**, *40*, 5361-5388.
- (36) Wu, H.; Chi, W.; Chen, Z.; Liu, G.; Gu, L.; Bindra, A.; Yang, G.; Liu, X.; Zhao, Y. Achieving

Amorphous Ultralong Room Temperature Phosphorescence by Coassembling Planar Small Organic Molecules with Polyvinyl Alcohol. *Adv. Funct. Mater.* **2019**, *29*, 1807243.

(37) Gmelch, M.; Thomas, H.; Fries, F.; Reineke, S. Programmable Transparent Organic Luminescent Tags. *Sci. Adv.* **2019**, *5*, eaau7310.

(38) Ogoshi, T.; Tsuchida, H.; Kakuta, T.; Yamagishi, T. A.; Mizuno, M. Ultralong Room-Temperature Phosphorescence from Amorphous Polymer Poly(Styrene Sulfonic Acid) in Air in the Dry Solid State. *Adv. Fun. Mat.* **2018**, *28*, 1707369.

(39) Gu, L.; Shi, H.; Gu, M.; Ling, K.; Ma, H.; Cai, S.; Song, L.; Ma, C.; Li, H.; Xing, G.; Hang, X.; Li, J.; Gao, Y.; Yao, W.; Shuai, Z.; An, Z.; Liu, X.; Huang, W. Dynamic Ultralong Organic Phosphorescence by Photoactivation. *Angew. Chem. Int. Ed.* **2018**, *57*, 8425-8431.

(40) Gahlaut, R.; Joshi, H. C.; Joshi, N. K.; Pandey, N.; Arora, P.; Rautela, R.; Suyal, K.; Pant, S. Luminescence Characteristics and Room Temperature Phosphorescence of Naphthoic Acids in Polymers. *J. Lumin.* **2013**, *138*, 122-128.

(41) Yuan, W. Z.; Shen, X. Y.; Zhao, H.; Lam, J. W. Y.; Tang, L.; Lu, P.; Wang, C.; Liu, Y.; Wang, Z.; Zheng, Q.; Sun, J. Z.; Ma, Y.; Tang, B. Z. Crystallization-Induced Phosphorescence of Pure Organic Luminogens at Room Temperature. *J. Phys. Chem. C* **2010**, *114*, 6090-6099.

(42) Gu, L.; Shi, H.; Bian, L.; Gu, M.; Ling, K.; Wang, X.; Ma, H.; Cai, S.; Ning, W.; Fu, L.; Wang, H.; Wang, S.; Gao, Y.; Yao, W.; Huo, F.; Tao, Y.; An, Z.; Liu, X.; Huang, W. Colour-Tunable Ultra-Long Organic Phosphorescence of a Single-Component Molecular Crystal. *Nat. Photonics* **2019**, *13*, 406-411.

(43) Más-Montoya, M.; Janssen, R. A. The Effect of *H*- and *J*-Aggregation on the Photophysical

and Photovoltaic Properties of Small Thiophene-Pyridine-DPP Molecules for Bulk-Heterojunction Solar Cells. *Adv. Funct. Mater.* **2017**, *27*, 1605779.

(44) Kashida, H.; Asanuma, H.; Komiyama, M. Alternating Hetero H Aggregation of Different Dyes by Interstrand Stacking from Two DNA-Dye Conjugates. *Angew. Chem. Int. Ed.* **2004**, *43*, 6522-6525.

(45) Nüesch, F.; Grätzel, M. H-Aggregation and Correlated Absorption and Emission of a Merocyanine Dye in Solution, at the Surface and in the Solid State. A Link between Crystal Structure and Photophysical Properties. *Chem. Phys.* **1995**, *193*, 1-17.

(46) Basak, S.; Nandi, N.; Baral, A.; Banerjee, A. Tailor-Made Design of J- or H-Aggregated Naphthalenediimide-Based Gels and Remarkable Fluorescence Turn On/Off Behaviour Depending on Solvents. *Chem. Comm.* **2015**, *51*, 780-783.

(47) Bailey, M.; Brown, C. J. The Crystal Structure of Terephthalic Acid. *Acta Crystallogr.* **1967**, *22*, 387-391.

(48) Ahmed, N. A. Theoretical Calculation of the Crystal Structure of Benzidine. *Indian J. Phys.* **1978**, *52*, 289-292.

(49) Wu, H.; Chen, Z.; Chi, W.; Kaur, B. A.; Gu, L.; Qian, C.; Wu, B.; Yue, B.; Liu, G.; Yang, G.; Zhu, L.; Zhao, Y. L. Structural Engineering of Luminogens with High Emission Efficiency both in Solution and the Solid State. *Angew. Chem. Int. Ed.* **2019**, *58*, 11419-11423.

(50) Filatov, M. A. Heavy-Atom-Free BODIPY Photosensitizers with Intersystem Crossing Mediated by Intramolecular Photoinduced Electron Transfer. *Org. Biomol. Chem.* **2020**, *18*, 10-27.

(51) Liu, R.; Gao, X.; Barbatti, M.; Jiang, J.; Zhang, G. Promoting Intersystem Crossing of a

Fluorescent Molecule via Single Functional Group Modification. *J. Phys. Chem. Lett.* **2019**, *10*, 1388-1393.

(52) Minaev, B. F. Calculation of the Spectra of Unsaturated Hydrocarbons by the Method of Complete Neglect of Differential Overlap of Configurational Excitation with an Account of the Spin-Orbit Interaction, *Soviet Phys. J.* **1971**, *14*, 644-649.

(53) Minaev, B. F. Calculation of the Benzene Molecule with Configuration Interaction, Spin-Orbit Interaction, and Complete Neglect of Differential Overlap, *Soviet Phys. J.* **1971**, *14*, 1116-1119.

(54) Bian, L.; Shi, H.; Wang, X.; Ling, K.; Ma, H.; Li, M.; Cheng, Z.; Ma, C.; Cai, S.; Wu, Q.; Gan, N.; Xu, X.; An, Z.; Huang, W. Simultaneously Enhancing Efficiency and Lifetime of Ultralong Organic Phosphorescence Materials by Molecular Self-Assembly. *J. Am. Chem. Soc.* **2018**, *140*, 10734-10739.

# TOC Graphic

